



Article

GsMAS1 Encoding a MADS-box Transcription Factor Enhances the Tolerance to Aluminum Stress in *Arabidopsis thaliana*

Xiao Zhang ^{1,2,3,4,5,†}, Lu Li ^{1,2,3,4,5,†}, Ce Yang ^{1,2,3,4,5}, Yanbo Cheng ^{1,2,3,4,5}, Zhenzhen Han ^{1,2,3,4,5}, Zhandong Cai ^{1,2,3,4,5}, Hai Nian ^{1,2,3,4,5,*} and Qibin Ma ^{1,2,3,4,5,*}

¹ The State Key Laboratory for Conservation and Utilization of Subtropical Agro-bioresources, South China Agricultural University, Guangzhou 510642, China; XZHANG916@163.com (X.Z.); 2019201044@njau.edu.cn (L.L.); yangce26@outlook.com (C.Y.); ybcheng@scau.edu.cn (Y.C.); zhenzhenH1@outlook.com (Z.H.); zdcai@stu.scau.edu.cn (Z.C.)

² The Guangdong Provincial Laboratory of Lingnan Modern Agricultural Science and Technology, South China Agricultural University, Guangzhou 510642, China

³ The Key Laboratory of Plant Molecular Breeding of Guangdong Province, College of Agriculture, South China Agricultural University, Guangzhou 510642, China

⁴ The Guangdong Subcenter of National Center for Soybean Improvement, College of Agriculture, South China Agricultural University, Guangzhou 510642, China

⁵ The National Engineering Research Center of Plant Space Breeding, South China Agricultural University, Guangzhou 510642, China

* Correspondence: hnian@scau.edu.cn (H.N.); maqibin@scau.edu.cn (Q.M.)

† These authors contributed equally to this work.

Received: 28 January 2020; Accepted: 14 March 2020; Published: 15 March 2020



Abstract: The MADS-box transcription factors (TFs) are essential in regulating plant growth and development, and conferring abiotic and metal stress resistance. This study aims to investigate *GsMAS1* function in conferring tolerance to aluminum stress in *Arabidopsis*. The *GsMAS1* from the wild soybean BW69 line encodes a MADS-box transcription factor in *Glycine soja* by bioinformatics analysis. The putative *GsMAS1* protein was localized in the nucleus. The *GsMAS1* gene was rich in soybean roots presenting a constitutive expression pattern and induced by aluminum stress with a concentration-time specific pattern. The analysis of phenotypic observation demonstrated that overexpression of *GsMAS1* enhanced the tolerance of *Arabidopsis* plants to aluminum (Al) stress with larger values of relative root length and higher proline accumulation compared to those of wild type at the AlCl₃ treatments. The genes and/or pathways regulated by *GsMAS1* were further investigated under Al stress by qRT-PCR. The results indicated that six genes resistant to Al stress were upregulated, whereas *AtALMT1* and *STOP2* were significantly activated by Al stress and *GsMAS1* overexpression. After treatment of 50 μM AlCl₃, the RNA abundance of *AtALMT1* and *STOP2* went up to 17-fold and 37-fold than those in wild type, respectively. Whereas the RNA transcripts of *AtALMT1* and *STOP2* were much higher than those in wild type with over 82% and 67% of relative expression in *GsMAS1* transgenic plants, respectively. In short, the results suggest that *GsMAS1* may increase resistance to Al toxicity through certain pathways related to Al stress in *Arabidopsis*.

Keywords: *GsMAS1*; MADS; Al stress; *Glycine Soja*; *Arabidopsis thaliana*

1. Introduction

The metal element most commonly found in soil is aluminum (Al) with an average content of about 7.45% [1]. Aluminum has a toxic effect on plants by limiting the growth of roots depending on its

existing form of Al^{3+} ion in acidic soil at $pH \leq 5$ [2,3]. The Al^{3+} ion at low concentrations (micromole levels) can quickly inhibit root growth resulting in reduced crop yield [4]. Therefore, it is believed that aluminum in acidic soil is the main factor limiting crop growth [5–8]; however, it is also a key factor limiting the growth and development of soybean [9].

The root tip is a sensitive part of the plant that responds to Al stress, and the initial manifestation of Al toxicity is that the elongation of the root tip is inhibited [8]. Previous reports found that the accumulation of Al^{3+} ion was mainly in 0–5 mm root tips with the richest section from the root tips of 2–3 mm length in crops such as wheat, maize, and peas [10–13]. Therefore, the root elongation and root Al^{3+} content in plants are useful in measuring plant aluminum toxicity [14].

The mechanisms of plant resistance to aluminum toxicity are external rejection and internal detoxification [15]. The mechanism of external rejection mainly takes place in the plant roots to prevent aluminum ions entering the root tip cells, whereas the detoxification mechanism has four main components: organic acid (OA) chelate aluminum ions, induced pH barrier, cell wall of aluminum fixation, and Al^{3+} transmembrane outflow. The aluminum toxicity caused by aluminum ions that have entered the plant cells can be alleviated mainly through the chelation of organic acids, the aluminum compartment in the vacuole and the combination of protein and other forms of internal detoxification [16–18]. Organic acid transporters including aluminum-activated malate transporter1 (ALMT1) and other members of the multidrug and toxic compound extrusion (MATE) citrate transporter family are reported to be involved in the external rejection of the aluminum toxicity mechanism in plants [19–22]. A recent study suggested that transcription factors also play certain roles in Al stress during the process of plant growth and development, for example, *WRKY46* as a transcriptional repressor of *ALMT1* regulated aluminum-induced malate secretion in Arabidopsis [23]; *WRKY22* improved tolerance to Al stress through activation of *FRDL4* and enhancement of citrate secretion in rice [24]. *STOP1* encoding a Cys2/His2 type zinc-finger transcription factor played critical roles in regulating ALMT1 and other genes to protect Arabidopsis from proton and aluminum toxicity [25–28], whereas several genes regulated by STOP1 can be activated by STOP2 under aluminum stress which is a STOP1 homolog in Arabidopsis [29]. In the meantime, homologous genes of *STOP1*, widely found in other plants such as *NtSTOP1* in tobacco, *GmSTOP1* in soybean and *SbSTOP1*-like genes in sweet sorghum, endow plants resistance to aluminum toxicity [30–32]. In addition, Agamous-like MADS-box protein AGL62 and NAC domain-containing protein 100 are the leading transcription factors (TFs) contributing flax tolerance to Al stress through regulation of plant growth and development [33].

The MADS family found in fungi, animals and plants possesses a highly conserved DNA-binding domain named MADS at N-terminal [34–36]. Based on the phylogenetic analysis, the MADS gene family created through a gene duplication occurred before the divergence of plants and animals can be divided into two large lineages of type I and type II [37,38]. In plants, the typical difference of MADS genes between type II and type I is that the plant MADS genes of type II have a k-domain [37,39]. The plant-special type II MADS has typical structures with MADS, I, K, and C domains, and is also known as MIKC MADS [40,41]. The MADS region contains a highly conserved element with approximately 60 amino acids and the MADS domain binds specifically to DNA [42,43]. The I region consists of between 30 and 35 amino acids containing more hydrophilic residues, and has the function of DNA specific binding [44]. The K region consists of 65–70 amino acids mediating the interaction between proteins [45]. The C region comprises about 30 hydrophobic amino acids, and the sequence and length of the lowest conservatism is to promote the formation of protein complexes, DNA binding and transcriptional activation [46–48].

The MADS family is an ancient and broadly studied transcription factor and plays essential roles in almost all developmental processes in plants, such as floral organ development [49,50], controlling the flowering time of plants [51], ovary development, seed-coat development [52,53], embryo development [54], determining the meristem [55], root growth [56], plant vegetative growth [57] and symbiosis induction [58], fruit development and ripening [59], silique architecture [60], modulating plant architecture and abscisic acid [61], and orchid reproductive development [62]. However,

less attention is paid to stresses regulated by MADS-box genes in plants. Recent studies have shown that the MADS-box genes regulate plant resistance to abiotic stresses [63]. In tomato, flower abnormalities induced by low temperatures are associated with expression changes of MADS-box genes including TM4, TM5, TM6 and TAG1 [64]. The *OsMADS26* overexpression can reduce the stress response to the external environment of transgenic rice and *Arabidopsis* [65]. Together with several other genes, *OsMADS87* could be a potential target for improving the thermal resilience of rice during reproductive development [66]. Moreover, *CaMADS* upregulated by abiotic stress in pepper functions as a positive stress-responsive transcription factor in the signaling pathways of cold, salt, and osmotic stress [67]. Genome-wide identification indicated that there were many MADS-box genes responding to abiotic stresses such as salt, drought, heat, and cold stress with differential expression levels in rice [68,69], *Brachypodium distachyon* seedlings [70], cabbage seedlings [71], *Brassica rapa* [70], and bread wheat [72]. Therefore, the recent reports suggested that MADS-box genes are key components of gene regulatory networks involved in responding to stress changes and developmental plasticity in plants [73].

In soybean, the MADS-box family with 163 putative members is also one of the biggest transcription factor superfamilies that regulates a variety of biological functions [38,72,74]. In recent decades, only several members of soybean MADS-box genes have been investigated such as *GmNMH7*, *GmMADS29*, *SOC1*, *GmGAL1*, *GmGAL2*, *GmAGL15*, *GmMADS28*, and *GmSEP1* [75–79]. Among them, *GmNMH7* is a photoperiod-dependent gene involved in flower development in soybean flowering reversion system [75]. *GmAGL1* plays important roles in both floral organ identity and fruit dehiscence, and promotes flowering through the photoperiod pathway [80,81]. A gain-of function MADS-box gene, *Dt2*, determines stem growth by repressing *Dt1* expression to promote early conversion of the shoot apical meristems into reproductive inflorescences [82]. Furthermore, *GmAGL15* can enhance the development of somatic embryogenesis both in *Arabidopsis* and soybean by promoting a dedifferentiated state, and partially by the control of ethylene biosynthesis and response [76,83–85]. Heterologous expression of *GmMADS28* in tobacco resulted in abnormal flower organ development in transgenic tobacco plants and promoted the flowering and dwarfing of transgenic plants in advance [77]. Mainly involved in the development of seeds in soybean, *GmSEP1* is related to the characteristics of floral organs [78]. Heterologous expression of *GmGAL2* accelerate flowering in *Arabidopsis* [79]. Other MADS-box genes such as *GmFLUa*, *GmAGL6*, and *GmSOC1* also play essential roles in reproductive transition, flowering, the floral initiation process and leaf development in soybean [86–88]. However, there are few studies on the MADS-box genes related to abiotic stresses and/or heavy metal stress in soybean. In this study, the *GsMAS1* encoding a MADS-box transcription factor was cloned from the wild soybean BW69 line. *GsMAS1* showing a constitutive expression pattern was accumulated in roots and induced by Al stress. Heterologous transformation of *GsMAS1* in *Arabidopsis* was used to investigate the molecular mechanism of the *GsMAS1* gene responding to aluminum stress.

2. Results

2.1. Bioinformatics Analysis of *GsMAS1* Gene

Based on data of the gene expression profile of the Al-resistant BW69 line of *Glycine soja* [89], an aluminum-induced gene from the gene expression profile was screened from the National Center for Biotechnology Information (NCBI) database using the sequence information. The sequence alignment showed that the gene had exactly the same sequence of open reading frame (ORF) as *GmNMHC5* (accession: NM_001254560.3) [90], which is located on soybean chromosome 13. The candidate gene was cloned from the BW69 line of *Glycine soja* by specific primers using the cDNA sequence of *GmNMHC5* as a reference. The candidate gene confirmed by the sequence results was then designated as *GsMAS1* (which encodes a MADS-box transcription factor tolerant to aluminum stress 1 in *Glycine soja*). The full cDNA sequence of *GsMAS1* from RT-PCR was 1000 bp with an ORF of 726 bp which encodes 241 amino acids with MW of 27.768 kDa (Additional file 1, Supplementary Materials). The *GsMAS1* gene

was induced by Al stress (25 μ M AlCl₃, 0.5 mM CaCl₂, pH 4.3) with over 2-fold expression level from the data of the gene expression profile [89,91]. The Basic Local Alignment Search Tool (BLAST) analysis of NCBI revealed that putative GsMAS1 protein has the structural characteristics of the MADS-box transcription factor with two conservative domains (Additional file 2, Figure S1). One of them is the MADS-box domain located at the position from the 2nd to the 77th amino acids; the other one is the k-box domain located at the 81st to the 169th amino acids. The structural characteristics showed that GsMAS1 protein belongs to myocyte enhancer factor 2 (MEF2)-like/Type II subfamily of MADS (MCM1, Agamous, Deficiens), and serum response factor (SRF) box family of eukaryotic transcriptional factors (Additional file 2, Figure S1). Multiple sequence alignments of MADS-box proteins (Type II subfamily) indicated that GsMAS1 protein is highly homologous with 59.27% identity compared to those of AtAGL21, BRADI_5g12437v3, GmAGL15, GsMADS23L1 and MTR_2g009890 proteins, whereas it is less homologous (45.52% identity) with those of AtAGL19, Dt2, OsMADS8, and OsMADS20 proteins (Figure 1a). The phylogenetic analysis also indicated differences among the members of the Type II subfamily of MADS-box transcription factors in plants. As shown in Figure 1b, 35 MADS-box TF proteins from soybean, Arabidopsis, rice, short-handled grass and alfalfa play diverse functions in regulation of male and female gametophyte morphogenesis (AtAGL13), floral activator (AtAGL19), flowering (GmAGL1, GmAP1, GmFULa, GmNMH7, OsMADS8), determinate floral meristems (AtAP1, AtSEP2); semi-determinate stem growth (GmSOC1), somatic embryogenesis (GmAGL15), cell divisions (AtSHP1, AtSHP2); age-related resistance (AtSVP), root development (AtAGL21, AtAGL44, GmNMHC5) (Figure 1b). The bioinformatics analysis indicated that GsMAS1 protein has a closer affinity with some MADS-box TF proteins, such as GsNMHC5, AtAGL21, and AtAGL44 proteins. The results suggest that GsMAS1 protein may function as a MADS transcription factor in root development and/or root traits in soybean.

2.2. Expression Patterns of GsMAS1 in Tissues and under Aluminum Stress

To detect the tissue expression pattern of GsMAS1, the samples of young root, leaf, and stem from the seedlings, and flower and pod at R₂ stage, were taken from the BW69 line of *Glycine soja*. The qRT-PCR was carried out to determine the expression levels of the GsMAS1 gene in different tissues and organs. The qRT-PCR result showed that the GsMAS1 gene presented a constitutive expression pattern and was abundant in roots, which was over twice of relative expression levels higher than those in other tissues and organs (Figure 2a).

To investigate the expression patterns of the GsMAS1 response to acidic aluminum stresses, the qRT-PCR was used to analyze the transcript abundance of GsMAS1 under AlCl₃ treatments designed with concentration gradients and time gradients. As shown in Figure 2b, GsMAS1 was upregulated during the process of AlCl₃ treatments (0.5 mM CaCl₂, pH 4.3). With the increase of AlCl₃ concentration, the transcription abundance of GsMAS1 increased gradually reaching the highest level at over three times that of the control at 50 μ M AlCl₃, and then declined to a lower level under high concentrations of AlCl₃ (Figure 2b). Under different time-gradient conditions, the transcripts of GsMAS1 was accumulated under AlCl₃ treatment (Figure 2c). In the absence of AlCl₃ (pH 4.3), the expression levels of GsMAS1 at 6 h and 12 h treatments showed no significant difference compared with those of the control (pH 5.8). However, the transcription abundance of GsMAS1 increased first and then decreased along with the treatment time of 50 μ M AlCl₃ (pH 4.3). The transcripts of GsMAS1 reached the highest level at 6 h treatment, 3.5 times of that of the control with no significant differences at other time points of AlCl₃ treatment (Figure 2c). The results suggest that GsMAS1 might play a potential role in Al stress.

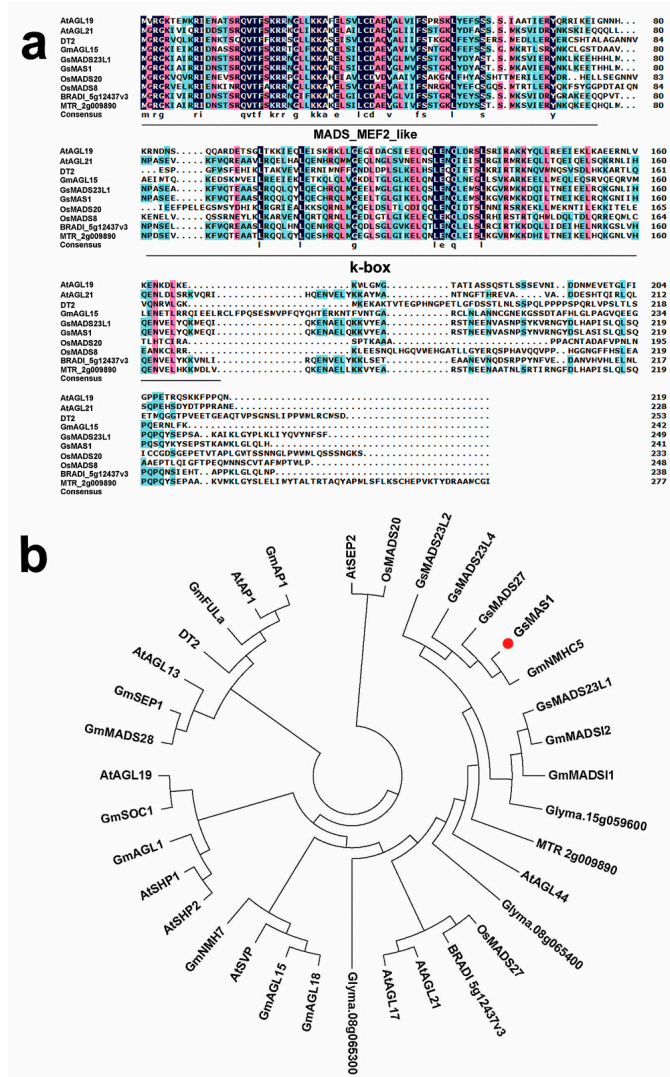


Figure 1. Homology analysis of GsMAS1 protein and other MADS-box transcription factors in plants. (a) Sequence alignment of GsMAS1 protein and MADS-box transcription factors. (b) Phylogenetic analysis of GsMAS1 and MADS-box transcription factors. The sequence alignment of amino acids was carried out by using the software DNAMAN6.0. The phylogenetic tree was constructed by the software MEGA (V6.0) with the neighbor-joining method. The amino acid sequences of MADS-box transcription factors are from the databases of the National Center for Biotechnology Information (NCBI) (<https://www.ncbi.nlm.nih.gov/>) and Phytozome (<http://phytozome.net/>). The information of accession number and species for MADS-box transcription factors is as follows. The proteins of AtAGL13 (AAC49081), AtAGL17 (OAP11731), AtAGL19 (AAG37901), AtAGL21 (NP_195507.1), AtAGL44 (NP_179033.1), AtAP1 (CAA78909), AtSHP1 (OAP06129), AtSEP2 (AAF61626), AtSHP2 (NP_850377), and AtSVP (OAP09056) are from *Arabidopsis thaliana*. The proteins of Dt2 (NP_001340272), Glyma.08g065300 (KRH42047), Glyma.08g065400 (XP_014634038), Glyma.15g059600 (KRH10635), GmAGL1 (NP_001304521), GmAGL15 (NP_001237033), GmAGL18 (XP_006575259), GmAP1 (XP_003547792), GmFULa (ahi43155), GmMADS28 (NP_001236390), GmMADSII1 (XP_014623536), GmMADSII2 (XP_025981482), GmNMH7 (NP_001236857), GmNMHC5 (XP_006593452), GmSEP1 (AAZ86071) and GmSOC1 (NP_001236377) are from *Glycine max*, whereas GsMADS23L1 (XP_028204324), GsMADS23L2 (XP_028187089), GsMADS23L4 (XP_028187090), GsMADS27 (RZB82838), and GsMAS1 are from wild soybean (*Glycine soja*). The proteins of OsMADS8 (Q9SAR1), OsMADS20 (Q2QQA3) and OsMADS27 (XP_015626695) are from *Oryza sativa*; MTR_2g009890 (AES63546) is from *Medicago truncatula*, BRADI_5g12437v3 (KQJ82998) is from *Brachypodium distachyon*.

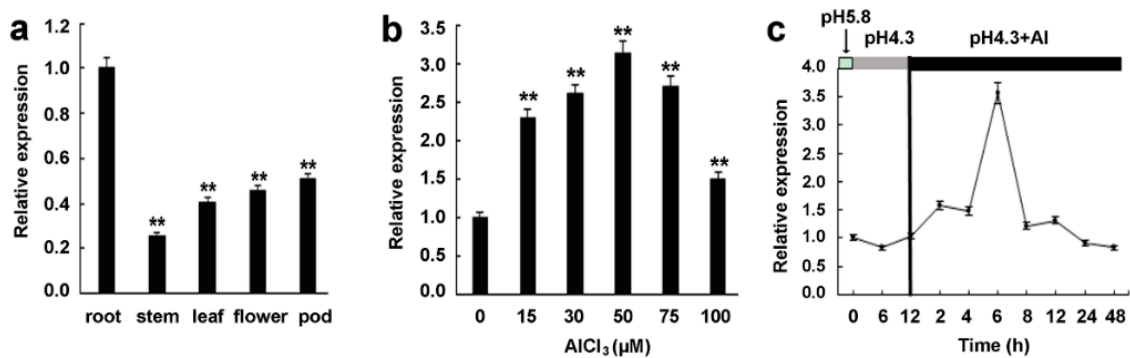


Figure 2. Expression patterns of *GsMAS1* in tissues and under acidic aluminum exposure. (a) Expression pattern analysis of *GsMAS1* in soybean tissues. Samples of roots, stems, and leaves are from young seedlings; flowers and pods were taken at the period of blooming and 15 days after soybean flowering, respectively. (b) Expression pattern of *GsMAS1* under the AlCl_3 treatments. After seed germination for two days, the seedlings of wild soybean (BW69 line) were transferred to AlCl_3 solutions, which were set as 0, 15, 30, 50, 75, and 100 μM (pH 4.3, 0.5 mM CaCl_2). After AlCl_3 treatments for 6 h, the 6-cm-long roots of seedlings were harvested to analyze the expression levels of *GsMAS1*. (c) Temporal expression pattern of *GsMAS1* under acidic aluminum exposure. The 2-day seedlings after germination were cultured in a solution of 0.5 mM CaCl_2 (pH 4.3) for 24 h, and then they underwent the 50 μM AlCl_3 treatment (pH 4.3, 0.5 mM CaCl_2). The 6-cm-long roots were taken from the seedlings at the processing time nodes of 2, 4, 6, 8, 12, and 24 h. The qRT-PCR was carried out to assess the transcript abundance of *GsMAS1* by the $2^{-\Delta\Delta\text{Ct}}$ method with *ACT3* as an internal control [92]. Three independent biological experiments were carried out to calculate the relative expression value of *GsMAS1*. Data are means \pm SE, and the asterisks (**) represent a significant difference ($p = 0.01$).

2.3. Subcellular Localization Analysis of *GsMAS1* Protein

To analyze the potential function of *GsMAS1* protein, subcellular localization analysis of *GsMAS1* protein was carried out in *Arabidopsis* protoplasts. As shown in Figure 3, the eGFP (enhanced green fluorescent protein) fluorescence signal in the protoplasts transformed with pYL322-d1-eGFP plasmid was clearly distributed throughout the cells, whereas the eGFP fluorescence signal in the protoplasts transformed with YL322-d1-eGFP-*GsMAS1* plasmid was only detected in the nucleus (Figure 3). The results demonstrated that *GsMAS1* protein was located in the nucleus.

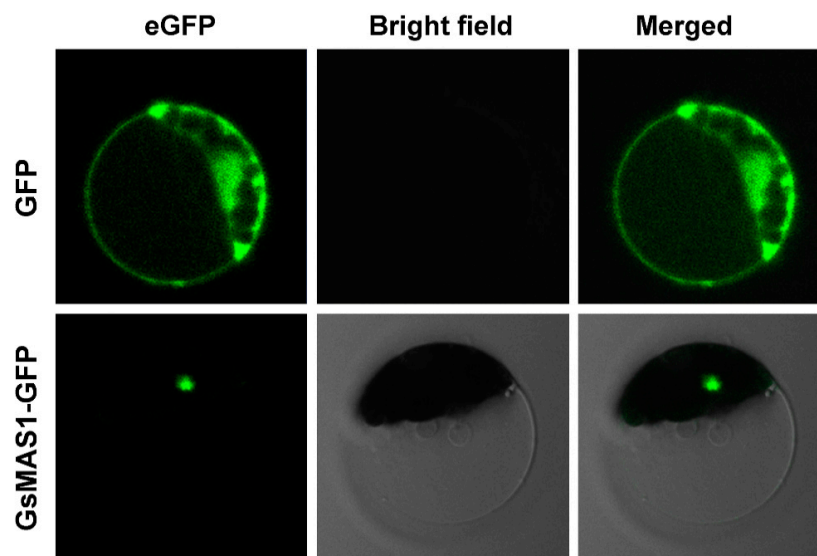


Figure 3. Subcellular localization of *GsMAS1* protein.

The vectors of pYL322-d1-eGFP and pYL322-d1-eGFP-GsMAS1 (eGFP: enhanced green fluorescent protein) were separately transformed into *Arabidopsis* protoplast cells using the heat-shock method. The vector-transformed cells cultured for 24 h were observed under a confocal scanning microscope (Leica, Germany) [50].

2.4. Molecular Identification of *GsMAS1* Transgenic *Arabidopsis* Lines

Thirteen *GsMAS1* transgenic lines in T₃ generation were underwent molecular identification to obtain homozygous lines. The PCR products of a specific band of 455 bp was detected in different *GsMAS1* transgenic lines (Figure 4a). The qRT-PCR was performed to determine the transcription levels of *GsMAS1* in wild type and transgenic lines using specific primers (Additional file 3, Table S1). Six homozygous lines of *GsMAS1* overexpression were further confirmed by qRT-PCR. The results indicated that the *GsMAS1* gene was overexpressed in transgenic lines with higher levels specifically in the lines of L4, L9, and L13. No RNA transcript of *GsMAS1* was detected in wild type of *Arabidopsis* (Figure 4b).

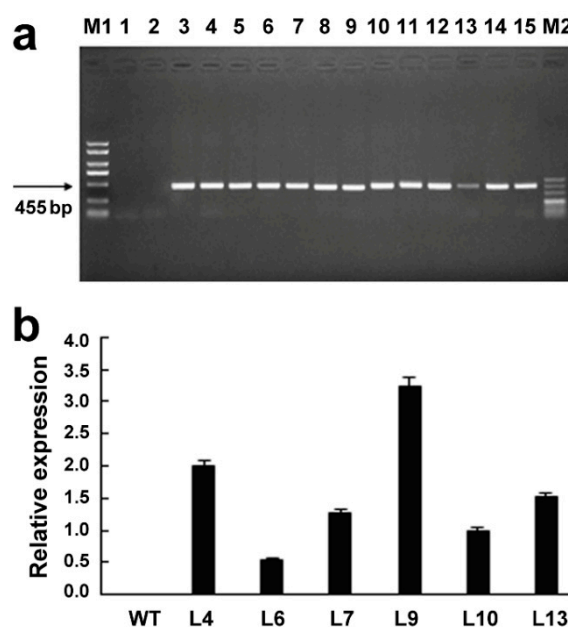


Figure 4. Molecular identification for *GsMAS1* transgenic lines in *Arabidopsis*. (a) PCR identification of *GsMAS1* transgenic plants. (b) qRT-PCR identification of *GsMAS1* transgenic lines. The 3-week-old seedlings of *Arabidopsis* were used to identify *GsMAS1* transgenic plant and lines. M1: DNA maker DL5000; M2: DNA marker DL500; Lanes 1–15: PCR products with different DNA templates set as ddH₂O for lane 1, genomic DNA from wide type for lane 2, genomic DNA from *GsMAS1* transgenic plants for lanes 3–15. WT: wild type of *Arabidopsis* Columbia-0; L4 to L13: six transgenic lines of *GsMAS1* in T₃ generation. Data are means \pm SE. Error bars represent the standard error of four replicates.

2.5. Phenotypic Analysis of *GsMAS1* Transgenic Lines

The three lines L4, L9, and L13, with a relatively high expression level of *GsMAS1*, were selected to investigate the acidic-resistant phenotypes of *GsMAS1* transgenic plants. The results showed the root elongations of *Arabidopsis* were inhibited under Al stress. With the increase of AlCl₃ concentration, the growth and development of roots were inhibited to a greater extent (Figure 5). The observation results indicated that there was no difference in elongation of taproots between *GsMAS1* transgenic lines and wild-type without AlCl₃ treatment (Figure 5a). The growth of the main roots of wild-type *Arabidopsis* was inhibited when treated with 50 μ M AlCl₃ (pH 4.5), whereas the main roots of transgenic *Arabidopsis* plants were significantly longer than those of wild type. The inhibition degree of principal roots increased significantly under the individual AlCl₃ treatments of 100 μ M, 150 μ M,

and 200 μM (Figure 5a,b). The relative root length (RRL) of the main root of *GsMAS1* transgenic lines was more than 70%, at 50 μM AlCl_3 , significantly higher than that of wild type (50%). Under the treatments of 100 μM and 150 μM AlCl_3 , the main root elongation of *Arabidopsis* was inhibited with a large decrease of RRLs both in wild type and transgenic plants. Compared to those of wild type, the roots of *GsMAS1* transgenic lines were less affected by Al stress with RRLs of over 50% and 40%, respectively (Figure 5a,b). At 200 μM AlCl_3 treatment, there was no difference in the elongation of the main roots between *GsMAS1* transgenic lines and wild type with RRLs at about 20% (Figure 5a,b). The results of phenotypic identification indicated that overexpression of the *GsMAS1* gene enhanced the tolerance of transgenic *Arabidopsis* to Al stress.

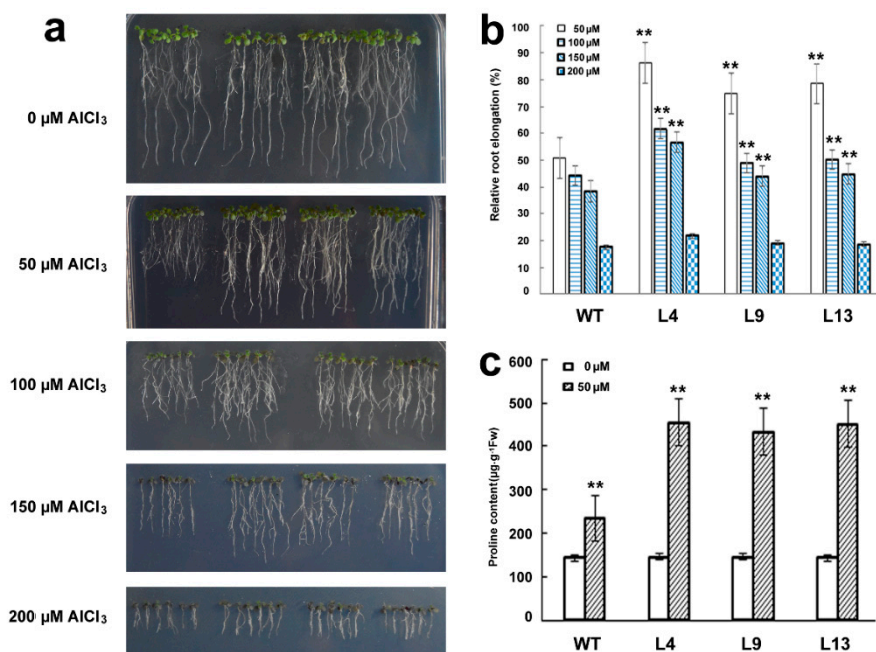


Figure 5. *GsMAS1* enhanced the resistance of *Arabidopsis* plants to Al stress (a) The phenotypes of *GsMAS1* transgenic lines tolerant to Al stress. (b) Statistical analysis of relative root elongation. (c) The determination of free proline content. WT: wild type of *Arabidopsis* (Col-0); L4, L9, L13: *GsMAS1* overexpression transgenic lines of T₃ generations. The two-day seedlings after seed germination were transferred to culture medium containing AlCl_3 (pH 4.3, 0.5 mM CaCl_2) at 0, 50, 100, 150, and 200 μM , individually. After being cultured for seven days, phenotypic images and contents of free proline for the *GsMAS1* transgenic lines were recorded and/or determined for statistical analysis. Data were represented as the means \pm SE of three biological replicates (Student's test, ** $p = 0.05$). The programs of Image J, SPSS20, and EXCEL2000 were used to measure and/or analyze the data.

2.6. Determination of Free Proline Content

Previous reports showed that proline accumulation can enhance maize tolerance to aluminum stress by minimizing accumulation of lipid peroxides [93]. In present study, in the absence of AlCl_3 treatment, the content of free proline was about $145 \mu\text{g}\cdot\text{g}^{-1}$ in both wild-type and *GsMAS1* transgenic plants with almost no difference (Figure 5c). Compared to the control, the content of free proline in *Arabidopsis* plants increased significantly at the treatment of 50 μM AlCl_3 . The content of free proline in wild type and *GsMAS1* transgenic *Arabidopsis* plants was about $230 \mu\text{g}\cdot\text{g}^{-1}$ and $440 \mu\text{g}\cdot\text{g}^{-1}$, respectively (Figure 5c). The determination result indicated that free proline was substantially accumulated in *GsMAS1* transgenic *Arabidopsis* under Al stress.

2.7. Expression Patterns of Al Stress Responsive Genes Regulated by *GsMAS1*

To make an investigation into the pathways regulated by *GsMAS1* under Al stress, some Al stress responding genes in Arabidopsis were used to test their expression patterns by qRT-PCR. The results can be put into four categories, according to the treatments with and without 50 μM AlCl_3 . Compared to those of wild type, three Al-upregulated genes of *AtMATE* (2.3-fold), *STOP1* (2.5-fold), and *PGIP2* (2.3-fold) were induced with relative expression abundances of over 2.3-fold in *GsMAS1* transgenic lines, whereas the RNA transcript of *WRKY46* sensitive to Al toxicity was less than half of that in the *GsMAS1* transgenic line. Under the treatment of 50 μM AlCl_3 , the RNA abundance of *AtMATE*, *AtALMT1*, *STOP1*, and *STOP2* in *GsMAS1* transgenic plants was much higher than that in wild type with over 27%, 82%, 19%, and 67% of relative expression, respectively (Figure 6). In addition, *AtALMT1* and *STOP2* under Al stress are significantly upregulated both in wild type and in *GsMAS1* transgenic plants with the largest absolute and relative expression (Figure 6). However, the RNA transcripts of *PGIP1* and *PGIP2* were less in *GsMAS1* transgenic lines than those in wild type of Arabidopsis at 50 μM AlCl_3 treatment (Figure 6). Furthermore, *WRKY46* and *ALS3* sensitive to Al stress had less RNA transcripts at 50 μM AlCl_3 treatment than those in the *GsMAS1* transgenic lines (Figure 6). All the results suggest that *GsMAS1* may enhance the tolerance to Al stress through the comprehensive effects of certain pathways in Arabidopsis.

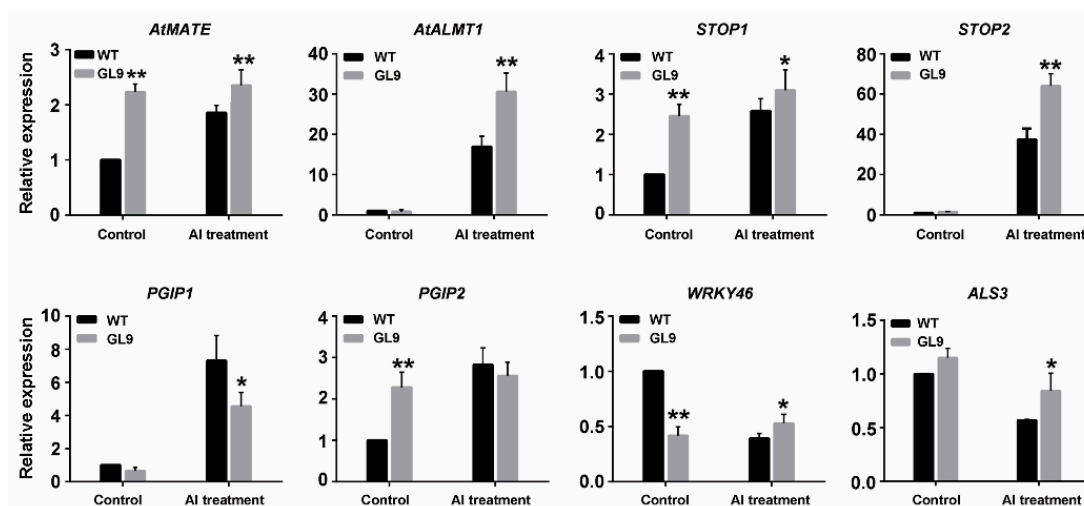


Figure 6. Expression patterns of Al stress responsive genes regulated by *GsMAS1*. Arabidopsis seeds of WT and the *GsMAS1* transgenic line L9 of T₃ generation were sown in 1/2 MS (Murashige-Skoog) culture media and cultured in the chamber room. The two-week-old seedlings were subjected to the treatment of solutions with or without 50 μM AlCl_3 (pH 4.3, 0.5 mM CaCl_2) for 24 h. The seedling samples from Arabidopsis plants were taken to extract total RNA. The transcription abundance of investigated genes was quantified by qRT-PCR using *ACT3* as the inner reference gene. The quantitative variation between the examined replicates was determined by the $2^{-\Delta\Delta C_t}$ method. The details of specific primers for *GsMAS1*, *ACT3* and measured genes are listed in Table S1 (Additional file 3). WT: wild type; GL9: *GsMAS1* transgenic line L9 of T₃ generation. The data were represented as the mean \pm SE of three biological replicates (t-test, ** $p = 0.05$).

3. Discussion

In this study, *GsMAS1* was cloned from the *Glycine soja* BW69 line. Sequence alignments indicated that putative *GsMAS1* protein is highly homologous, with over 59% identity compared to those of *AtAGL21*, *BRADI_5g12437v3*, *GmNMHC5*, *GmAGL15*, *GsMADS23L1* and *MTR_2g009890* proteins (Figure 1a). The *GsMAS1* protein possesses the typical structural features of a MADS-box protein with a conserved MEF2 MADS domain and the k-box domain, which was consistent with the structure of the Type II subfamily of MADS-box transcription factors in plants [79]. The *GsMAS1* protein was localized

to the nucleus of Arabidopsis protoplast cells (Figure 3). A similar result was found in GmNMHC5 protein, which shares 100% amino acids identity with GsMAS1 protein [90]. Therefore, we speculated that GsMAS1 protein may function as a MADS-box transcription factor and play certain roles in plants.

The phylogenetic analysis showed that GsMAS1 protein including GmNMHC5 protein belongs to the Type II subfamily of MADS-box members under the branch of the AGL17/AGL21 subfamily with a closer relationship to MADS TF proteins in soybean (Figure 1b) [90]. It has been reported that the members of AGL17 subfamily play significant roles in root system architecture construction and/or root development [94]. The *GsMAS1* gene, which is a constitutive expression gene with the richest transcripts in soybean root [90] (Figure 2), was quickly upregulated by AlCl₃ treatment (Figure 2). Therefore, we speculate that *GsMAS1* is involved in the regulation of plant tolerance to Al stress.

To further investigate its function, *GsMAS1* was transformed into Arabidopsis to obtain the homologous lines to verify the Arabidopsis tolerance to Al stress. Compared with the control treatment, the elongation of main roots of wild-type and transgenic Arabidopsis plants was inhibited to a serious degree by aluminum stress along with the increase of AlCl₃ concentration (Figure 5a). Under 50 μM AlCl₃ treatment, the root lengths of transgenic Arabidopsis with a relative root elongation (RRE) of over 70% were larger than those of wild type with an RRE of 50%. Significant differences were also found between the AlCl₃ treatments of 100 μM and 150 μM AlCl₃ (Figure 5a). Similar resistant phenotypes to abiotic stress were also investigated in other TF genes in soybean. For example, *GmWRKY16* enhanced the tolerance of transgenic Arabidopsis plants to drought and salt stresses through an ABA-mediated pathway in *Arabidopsis thaliana* [95]. In this study, the contents of proline in *GsMAS1* transgenic lines and wild type were also determined to investigate the response of Arabidopsis plants to Al stress, and the results were consistent with those of previous reports (Figure 5c) [93,95]. The results suggest that *GsMAS1* transgenic Arabidopsis may promote plant tolerance to Al stress to a certain extent by the content changes of free proline accumulation.

In the present study, several Al-stress-response genes were used to investigate the molecular basis of *GsMAS1* tolerance to Al stress. Six Al-stress up-regulating genes and two Al-stress down-regulating genes indicated that they have different responses to Al stress with different RNA abundance, both in *GsMAS1* transgenic plants and wild type, under Al stress. On the basis of expression patterns, we speculate that *STOP1*, *AtALMT1*, and *STOP2* are the key genes, which may play a critical role in *GsMAS1* regulation pathways (Figure 6). The qRT-PCR analysis showed that *STOP1* was activated by *GsMAS1* and Al stress (Figure 6), which plays essential roles in proton and aluminum toxicities by regulating multiple genes in Arabidopsis [25–27,29,30]. The *AtALMT1* gene, which is the target gene regulated by *STOP1* and the *STOP2* gene, which is a homolog of *STOP1*, were significantly induced by *GsMAS1* expression in transgenic Arabidopsis plants with much higher transcription levels (Figure 6) [19–22,29]. Previous reports indicated that *STOP2* confers Al and low pH tolerance by activating transcription of several genes regulated by *STOP1* in Arabidopsis [29]. *AtMATE* and *AtALMT1* in Al stress response identified through work on *STOP1* were upregulated by *GsMAS1* overexpression under the treatment of AlCl₃ (Figure 6), which conferred aluminum tolerance in Arabidopsis independently by accumulation of aluminum-activated citrate and malate [19–22]. Moreover, *PGIP1* and *PGIP2*, which were downregulated by *STOP2* and associated with cell wall stabilization at low pH [29], were activated being expressed in *GsMAS1* transgenic lines under aluminum stress (Figure 6). As a negative regulator of *ALMT1*, *WRKY46* regulated aluminum-induced malate secretion in Arabidopsis [23], whereas *ALS3* protected the growing root from Al toxicity by redistributing accumulated Al away from sensitive tissues [96]. The RNA transcripts of *WRKY46* and *ALS3* both in wild type and *GsMAS1* transgenic lines under aluminum stress were less than those in the treatment of the control (Figure 6). The results indicated that *GsMAS1* enhanced resistance to Al toxicity by certain pathways in Arabidopsis. In addition, three genes, *AtMATE*, *STOP1*, and *PGIP2*, were upregulated by *GsMAS1* in Arabidopsis (Figure 6), which suggested that *GsMAS1* might participate in the regulation of other potential functions of the MADS genes in Arabidopsis.

Furthermore, phylogenetic analysis showed that GsMAS1 protein holds the same sequence as GmNMHC5 protein (Figure 1b). However, the non-coding sequences of GsMAS1 are different from those of GmNMHC5 (Additional file 1, Supplementary Materials). The GmNMHC5 gene induced by sucrose with a temporal and spatial expression pattern was rich in roots, nodules, and pods. Overexpression of GmNMHC5 significantly accelerated lateral root development and nodulation in soybean [90]. Moreover, rich in roots and pods, GsMAS1 enhanced resistance to Al stress in transgenic Arabidopsis without phenotype of root development (Figure 5a). The phenotype differences between soybean and Arabidopsis may be due to the differential activations and/or divergent pathways regulated by GsMAS1 and GmNMHC5 proteins, respectively. Therefore, further studies could focus on the potential roles in the regulation of GsMAS1 promoter and the target genes interacting with GsMAS1.

The MADS family is one of the biggest transcription factor superfamilies and plays a fundamental role in almost every developmental process in soybean. Shu et al. (2013) found that there were 106 putative MADS-box genes by genome-wide survey and expression analysis, 72 genes among them being type II MADS-box TFs [72]. Fan et al. (2013) obtained 163 MADS genes from soybean genome by genome-wide expression analysis, and 115 MADS-box genes among them play potential function in seed development [36]. In recent years, researches on the MADS-box genes have focused on the regulations of plant growth and development, and flowering in soybean [90]. However, there are few reports for soybean MADS-box transcription factors/regulators related to abiotic and heavy metal stresses. More and more MADS-box transcription factors found in succession by the means of bioinformatics and genomics-wide analysis will provide the database to make profound studies for their roles of MADS-box TFs in the response to Al stress in soybean. Consequently, further study on the function of the GsMAS1 gene will enrich our understanding of the mechanism of acid-tolerant aluminum in plants.

4. Materials and Methods

4.1. Plant Materials and Growth Conditions

The BW69 line of *Glycine soja* and Columbia-0 (Col-0) ecotype of Arabidopsis were both propagated and preserved by the Guangdong Subcenter of the National Center for Soybean Improvement (Guangzhou, China). The seeds of the BW69 line were germinated in vermiculite with room temperature set at 28/26 °C and the light time set as 14 h-light/10 h-dark under a light intensity of 110 $\mu\text{mol}/(\text{m}^2\cdot\text{s})$ [89,92]. The Arabidopsis seeds of Col-0 ecotype were germinated in nutrient soil (substrate: vermiculite = 3:1) with room temperature set as 24/22 °C and the light time set as 16 h-light/8 h-dark under a light intensity of 120 $\mu\text{mol}/(\text{m}^2\cdot\text{s})$ [89,92].

4.2. Bioinformatics Analysis of GsMAS1 Gene

The sequencing data from the gene expression profile resistant to acidic aluminum of the *Glycine soja* BW69 line were used to find the potential sequence of the GsMAS1 gene. Sequence Blast was carried out in the NCBI (<http://www.ncbi.nlm.nih.gov/>) and Phytozome (<http://phytozome.net/>) databases to obtain the putative sequence of GsMAS1 for gene cloning, predicted domains of GsMAS1 protein and the sequences of amino acids for the related homologous proteins. The software package DNAMAN was used to perform homologous sequence alignment, whereas MEGA (V6.0) software (Tokyo Metropolitan University, Tokyo, Japan) was used to analyze phylogenetic relations among all the MADS-box transcription factors [92].

4.3. Analysis of GsMAS1 Expression Patterns

To analyze tissue expression pattern of GsMAS1, the seeds of the BW69 line with cut-coat on the back of hilum were sowed in the farm field of the campus at South China Agricultural University. When the wild soybean plants began to pod, the samples of flower and young pod were taken at the R₂ stage [89,92], and then frozen in liquid nitrogen and stored at -80 °C in an ultra-low temperature

refrigerator [92]. The samples of root, stem, and leaf were taken from the young seedlings of the BW69 line [89].

To investigate the response of *GsMAS1* to acid aluminum stress, the cut-coat seeds of the BW69 line were prepared and sterilized with 3% hydrogen peroxide for 30 s, rinsed 3–4 times with distilled water and sprouted in autoclaved vermiculite. When the leaf blades of soybean seedlings had completely unfolded, the seedling vermiculite on the surface of leaves was rinsed with ultrapure water. The cleaned seedlings pre-cultured in nutrient solution (pH 5.8) for 48 h were then transferred to a simple calcium solution of 0.5 mM CaCl_2 (pH 4.3) for pretreatment after 24 h. The concentrations of AlCl_3 (0.5 mM CaCl_2 , pH 4.3) solution were set as 0 μM , 15 μM , 30 μM , 50 μM , 75 μM , and 100 μM individually [97]. Eighteen seedlings were treated at each concentration for three replicates. Samples of 2 mm-long root tips were harvested after AlCl_3 treatment for 6 h, wrapped in foil, frozen in liquid nitrogen, and then stored at -80°C in an ultra-low temperature refrigerator.

To detect the temporal expression pattern of *GsMAS1*, the seedlings of the BW69 line were prepared in 0.5 mM CaCl_2 solution (pH 4.3) in the same way above and separately sampled at 0 h, 6 h, and 12 h. During the treatment process of 50 μM AlCl_3 (0.5 mM CaCl_2 , pH 4.3) for 48 h, the samples of 2 mm-long root tips from young seedlings were taken at 2 h, 4 h, 6 h, 8 h, 12 h, 24 h, and 48 h, individually [97], and then frozen in liquid nitrogen and stored at -80°C in an ultra-low temperature refrigerator.

4.4. Real-time Quantitative PCR

TransZol Up (Trangen Biotech, Beijing, China) was used to extract total RNA from different samples. First-strand cDNA was synthesized using EasyScript One-Step gDNA Removal and cDNA Synthesis SuperMix Kit using 1.5 μg RNA as a template. Quantitative real-time PCR was performed on a CFX96 Real-Time PCR Detection System device (Bio-Rad, Hercules, CA, USA) using the SsoFast EvaGreen Supermix Kit (Bio-Rad, Shanghai, China). All the reactions were carried out in 20 μL volumes containing 1 μL cDNA as a template. Primers are listed in Table S1 (Additional file 3) for ACT3-F and ACT3-R, q*GsMAS1*-F and q*GsMAS1*-R, and At-TUB-F and At-TUB-R. The following procedure was used for qRT-PCR: 94°C for 3 min; 40 cycles of denaturation at 94°C for 10 s, annealing at 59°C for 10 s, elongation at 72°C for 30 s. Data were analyzed using the $2^{-\Delta\Delta\text{CT}}$ method as described above [98].

4.5. Subcellular Localization Analysis of *GsMAS1* Protein

To investigate the subcellular localization of *GsMAS1* protein, the full-length cDNA without the stop codon of *GsMAS1* was inserted into the restriction sites of *KpnI* and *BamHI* to construct a pYL322-d1-eGFP-*GsMAS1* vector using the specific primers of C-*GsMAS1*-F and C-*GsMAS1*-R (Additional file 3, Table S1) [92]. The CDS (coding sequence) sequence of *GsMAS1* was inserted into the downstream of the GFP sequence by recombinant DNA technology. The vectors pYL322-d1-eGFP and pYL322-d1-eGFP-*GsMAS1* were then transformed into *Arabidopsis* protoplasts by a PEG-mediated method and cultured in the dark for two days [21]. The expression signal of GFP was observed and photographed under a confocal laser scanning microscope (Carl Zeiss, Oberkochen, Germany).

4.6. Cloning of *GsMAS1* Gene

The gene of Gene ID: 100,805,092 was selected from the gene expression profile resistant to aluminum stress of the *Glycine soja* BW69 line, and then the NCBI database was used to search for the sequence information for the candidate gene. According to the obtained sequence from the database of NCBI, the CDS sequences of the *GsMAS1* gene were amplified from cDNA of *Glycine soja* BW69 roots with specific primers *GsMAS1*-F and *GsMAS1*-R (Additional file 3, Table S1). Total RNA extraction, cDNA generation and RT-PCR amplification were carried out according to the methods described in detail previously [89]. The PCR product was purified by 1% agarose gel electrophoresis (GenStar Kit, Genstar Development Company, Calgary, AB, Canada) and then purified by Tiangen Rapid DNA Ligation Kit (Beijing, China). The purified fragment for *GsMAS1* was inserted into the multi-cloning site of pLB vector to construct pLB-*GsMAS1* vector with the reference of pLB zero background rapid

cloning kit (TIANGEN, Beijing, China). Clones of *E. coli* transformed with the pLB-GsMAS1 vector using the heat-shock method were identified by PCR and enzyme digestion by methods previously described in detail [89]. The positive clones were sequenced to obtain the full cDNA sequence of GsMAS1 (Sangon, Shanghai, China).

4.7. Construction of Plant Expression Vector

According to the sequence information, the ORF sequence of 723 bp length of the GsMAS1 gene was inserted into the *Xba*I and *Sac*I sites of plant-expression vector pTF101.1-GFP by homologous recombination technology to construct the fusion expression vector of pTF101.1-GsMAS1. The expression of the GsMAS1 gene was driven by the 35 S promoter in *E. coli* cells. The experimental operations PCR amplification, DNA segregation and purification, and fusion vector transformation for the target fragment were carried out by the methods for GsMAS1 cloning described above in detail. All the monoclonal clones were identified by PCR and restriction enzyme digestion. The positive clones were sent to a biotechnology company (Sangon, Shanghai, China) for sequencing, and the sequence result was then confirmed using the NCBI database [91].

4.8. Heterologous Expression of GsMAS1 in Arabidopsis

The ORF of GsMAS1 was inserted into the *Xba*I and *Sac*I sites to form a pTF101.1-GsMAS1 vector using the primers p-GsMAS1-F and p-GsMAS1-R (Additional file 3, Table S1) by the homologous recombination method. The recombinant plasmids were transformed into the competent cells of *Agrobacterium tumefaciens* GV3101 by the electroporation method. Arabidopsis genetic transformation was carried out using the floral dip method to obtain transgenic plants [99]. After the siliques matured, seeds of T₀ generation were harvested, dried and then vernalized at 4 °C for further identification and generation. When two pieces of true leaves are fully unfolded, the T₁ Arabidopsis seedlings were initially screened with 10 mg/L glufosinate and then further identified at the DNA and RNA levels [89]. After the positive seedlings of transgenic Arabidopsis plants matured, the seeds were individually harvested to form transgenic lines. Homozygous transgenic lines of T₃ generation by herbicide application of 10 mg/L glufosinate and PCR identification were produced to investigate the GsMAS1 phenotypes tolerant to Al stress [89].

4.9. Phenotypic Identification of GsMAS1 Transgenic Lines

In the present study, 13 positive transgenic plants obtained in succession by herbicide application and PCR identification were propagated to gain the GsMAS1 transgenic lines of T₃ generation. To obtain homozygous lines, the Arabidopsis seedlings in T₃ generation of 13 GsMAS1 transgenic lines underwent molecular identification. The specific band of PCR products detected by agarose gel electrophoresis indicated that the ORF sequence of GsMAS1 was successfully inserted into the Arabidopsis genome. The Arabidopsis seeds of wild-type and GsMAS1 transgenic lines of T₃ generation sterilized with 70% ethanol for 2 min, 1% sodium hypochlorite for 5 min, and sterilized water three times were spotted on 1/2 MS solid medium (pH 5.8) in one-time culture dish sealed with the microporous air-permeable sealer. After incubation at 4 °C for 2–3 days, Arabidopsis seeds in all the culture dishes were placed in a vertical light incubator with the conditions of light time 16 h/8 h (day/night), temperature 22–24 °C, humidity 50%. When the root length of Arabidopsis plants was up to about 1 cm, the seedlings with almost the same root length were selected and transferred to 1/2 MS solid agar medium containing different AlCl₃ concentrations set as 0 μM, 50 μM, 100 μM, 150 μM, and 200 μM (0.5 mM CaCl₂, pH 4.5). After being cultured for 7 days, all the treatments for phenotypes tolerant to Al stress were photographed with the root length being measured by Image J software [100]. The index of relative elongation of main root (%) was used to evaluate root changes of Arabidopsis seedlings under Al stress [100]. The seedlings under the treatments of 0 μM and 50 μM AlCl₃ of GsMAS1 transgenic lines and wild-type plants were used to determine contents of free proline by the methods described in detail previously [97].

4.10. Statistical Analysis

All the experiments for the analysis of expression pattern, molecular identification, phenotype tolerant to Al stress and regulation pathway of *GsMAS1* were carried out with three independent biological replicates. All the data were presented as mean \pm SE. An LSD test ($p = 0.05$ or $p = 0.01$) was carried out to investigate the differences between observation values [89].

5. Conclusions

We investigated a soybean *GsMAS1* gene encoding a MADS-box transcription factor from BW69 line of *Glycine soja*. The *GsMAS1* gene was induced by Al stress and rich in roots with a constitutive expression pattern in soybean. The *GsMAS1* protein was located in the nucleus. Ectopic overexpression of *GsMAS1* in *Arabidopsis* enhanced the tolerance of transgenic plants to Al stress with free proline accumulation. The molecular investigation indicated that the enhanced tolerance to Al toxicity of *GsMAS1* transgenic *Arabidopsis* was caused by the comprehensive role played by some critical genes in responding to Al stress. The results suggested that *GsMAS1* protein may increase resistance to Al toxicity through certain pathways related to Al stress in *Arabidopsis* and provide a scientific basis for soybean molecular breeding.

Supplementary Materials: Supplementary materials can be found at <http://www.mdpi.com/1422-0067/21/6/2004/s1>. Sequence information of CDS and amino acid. Figure S1: The putative domains of the *GsMAS1* protein. Table S1: List of the primers in present study.

Author Contributions: Conceptualization, X.Z. and Q.M.; Data Curation, X.Z., L.L., C.Y., and Q.M.; Formal analysis, C.Y.; Funding acquisition, H.N. and Q.M.; Methodology, X.Z., L.L., C.Y., and Y.C.; Project administration, X.Z.; Validation, L.L., C.Y., Y.C., Z.H., and Z.C.; Writing—original draft, X.Z.; Writing—review and editing, X.Z., L.L., H.N., and Q.M. All authors have read and agreed to the published version of the manuscript.

Funding: This work was supported by the grants from the Major Project of New Varieties Cultivation of Genetically Modified Organisms (2016ZX08004002–007), the National Natural Science Foundation of China (31771816, 31971965), the Key Projects of International Scientific and Technological Innovation Cooperation among Governments under National Key R & D Plan (2018YFE0116900); the China Agricultural Research System (CARS-04-PS09), the Project of Science and Technology of Guangzhou (201804020015) and the Research Project of the State Key Laboratory for Conservation and Utilization of Subtropical Agro-Bioresources (4100-M13024).

Acknowledgments: The authors are very grateful to Yaoguang Liu (South China Agricultural University, China) for providing us the pYL322-d1-eGFP vector. We would also like to thank the MDPI team for their great help in improving the language of the present manuscript.

Conflicts of Interest: The authors declare that they have no competing interests.

Abbreviations

| | |
|---------|--|
| Gs | Glycine Soja |
| MML | MADS_MEF2_like |
| BW69 | Glycine Soja line |
| DEF 125 | DEFICIENS 125 |
| SQUA | SQUAMOSIA |
| TM4 | tomato MADS-box gene no. 4 |
| TM5 | tomato MADS-box gene no. 5 |
| TM6 | tomato MADS-box gene no. 6 |
| TAG1 | tomato AGAMOUS gene no. 1 |
| PEG | polyethylene glycol |
| CDS | coding sequence |
| ORF | open reading frame |
| Al | aluminum |
| NCBI | the National Center for Biotechnology Information |
| WT | wild type of <i>Arabidopsis</i> Columbia-0 (Col-0) |
| LSD | Least-Significant Difference |

References

1. Tesfaye, M.; Temple, S.J.; Allan, D.L.; Vance, C.P.; Samac, D.A. Overexpression of malate dehydrogenase in transgenic alfalfa enhances organic acid synthesis and confers tolerance to aluminum. *Plant Physiol.* **2001**, *127*, 1836–1844. [[CrossRef](#)] [[PubMed](#)]
2. Hoekenga, O.A.; Vision, T.J.; Shaff, J.E.; Monforte, A.J.; Lee, G.P.; Howell, S.H.; Kochian, L.V. Identification and characterization of aluminum tolerance loci in *Arabidopsis* (*Landsberg erecta* × *Columbia*) by quantitative trait locus mapping. A physiologically simple but genetically complex trait. *Plant Physiol.* **2003**, *132*, 936–948. [[CrossRef](#)] [[PubMed](#)]
3. Kochian, L.V.; Hoekenga, O.A.; Piñeros, M.A. How do crop plants tolerate acid soils? Mechanisms of aluminum tolerance and phosphorous efficiency. *Annu. Rev. Plant Biol.* **2004**, *55*, 459–493. [[CrossRef](#)] [[PubMed](#)]
4. Ma, J.; Ryan, P.R.; Delhaize, E. Aluminium tolerance in plants and the complexing role of organic acids. *Trends Plant Sci.* **2001**, *6*, 273–278. [[CrossRef](#)]
5. Pandey, P.; Srivastava, R.K.; Dubey, R.S. Salicylic acid alleviates aluminum toxicity in rice seedlings better than magnesium and calcium by reducing aluminum uptake, suppressing oxidative damage and increasing antioxidative defense. *Ecotoxicology* **2013**, *22*, 656–670. [[CrossRef](#)]
6. Alvimmm, M.; Ramos, F.; Oliveira, D.; Isaias, R.; Franca, M. Aluminium localization and toxicity symptoms related to root growth inhibition in rice (*Oryza sativa* L.) seedlings. *J. Biosci.* **2012**, *37*, 1079–1088. [[CrossRef](#)]
7. Sapra, V.; Mebrahtu, T.; Mugwira, L. Soybean germplasm and cultivar aluminum tolerance in nutrient solution and bladen clay loam soil. *Agronomy* **1982**, *74*, 687–690. [[CrossRef](#)]
8. Chandran, D.; Sharopova, N.; Ivashuta, S.; Gantt, J.S.; VandenBosch, K.A.; Samac, D.A. Transcriptome profiling identified novel genes associated with aluminum toxicity, resistance and tolerance in *Medicago truncatula*. *Planta* **2008**, *228*, 151–166. [[CrossRef](#)]
9. Lazof, D.B.; Goldsmith, J.G.; Rufty, T.W.; Linton, R.W. Rapid uptake of aluminum into cells of intact soybean root tips. A microanalytical study using secondary ion mass spectroscopy. *Plant Physiol.* **1994**, *106*, 1107–1114. [[CrossRef](#)]
10. Sivaguru, M.; Baluška, F.; Volkmann, D.; Felle, H.H.; Horst, W.J. Impacts of aluminum on the cytoskeleton of the maize root apex. short-term effects on the distal part of the transition zone. *Plant Physiol.* **1999**, *119*, 1073–1082. [[CrossRef](#)]
11. Maron, L.G.; Piñeros, M.A.; Guimarães, C.T.; Magalhaes, J.V.; Pleiman, J.K.; Mao, C.; Shaff, J.; Belicuas, S.N.; Kochian, L.V. Two functionally distinct members of the MATE (multi-drug and toxic compound extrusion) family of transporters potentially underlie two major aluminum tolerance QTLs in maize. *Plant J.* **2010**, *61*, 728–740. [[CrossRef](#)] [[PubMed](#)]
12. Motoda, H.; Kano, Y.; Hiragami, F.; Kawamura, K.; Matsumoto, H. Morphological changes in the apex of pea roots during and after recovery from aluminium treatment. *Plant Soil* **2010**, *333*, 49–58. [[CrossRef](#)]
13. Kopittke, P.M.; McKenna, B.A.; Karunakaran, C.; Dynes, J.J.; Arthur, Z.; Gianoncelli, A.; Kourousias, G.; Menzies, N.W.; Ryan, P.R.; Wang, P. Aluminum complexation with malate within the root apoplast differs between aluminum resistant and sensitive wheat lines. *Front. Plant Sci.* **2017**, *8*, 1377. [[CrossRef](#)] [[PubMed](#)]
14. Kong, X.; Zhang, M.; Xu, X.; Li, X.; Li, C.; Ding, Z. System analysis of microRNAs in the development and aluminium stress responses of the maize root system. *Plant Biotechnol. J.* **2014**, *12*, 1108–1121. [[CrossRef](#)] [[PubMed](#)]
15. Matsumoto, H. Cell biology of aluminum toxicity and tolerance in higher plants. *Int. Rev. Cytol.* **2000**, *200*, 1–46. [[PubMed](#)]
16. Ma, J.F. Role of organic acids in detoxification of aluminum in higher plants. *Plant Cell Physiol.* **2000**, *41*, 383–390. [[CrossRef](#)]
17. Ryan, P.; Delhaize, E.; Jones, D. Function and mechanism of organic anion exudation from plant roots. *Annu. Rev. Plant Physiol. Plant Mol. Biol.* **2001**, *52*, 527–560. [[CrossRef](#)]
18. Kochian, L.V.; Pineros, M.A.; Liu, J.; Magalhaes, J.V. Plant adaptation to acid soils: The molecular basis for crop aluminum resistance. *Annu. Rev. Plant Biol.* **2015**, *66*, 571–598. [[CrossRef](#)]
19. Kobayashi, Y.; Hoekenga, O.A.; Itoh, H.; Nakashima, M.; Saito, S.; Shaff, J.E.; Maron, L.G.; Pineros, M.A.; Kochian, L.V.; Koyama, H. Characterization of *AtALMT1* expression in aluminum-inducible malate release and its role for rhizotoxic stress tolerance in *Arabidopsis*. *Plant Physiol.* **2007**, *145*, 843–852. [[CrossRef](#)]

20. Kobayashi, Y.; Lakshmanan, V.; Kobayashi, Y.; Asai, M.; Iuchi, S.; Kobayashi, M.; Bais, H.P.; Koyama, H. Overexpression of *AtALMT1* in the *Arabidopsis thaliana* ecotype Columbia results in enhanced Al-activated malate excretion and beneficial bacterium recruitment. *Plant Signal. Behav.* **2013**, *8*, e25565. [[CrossRef](#)]
21. Liu, J.; Magalhaes, J.V.; Shaff, J.; Kochian, L.V. Aluminum-activated citrate and malate transporters from the MATE and ALMT families function independently to confer Arabidopsis aluminum tolerance. *Plant J.* **2009**, *57*, 389–399. [[CrossRef](#)]
22. Liu, J.; Luo, X.; Shaff, J.; Liang, C.; Jia, X.; Li, Z.; Magalhaes, J.; Kochian, L.V. A promoter-swap strategy between the *AtALMT* and *AtMATE* genes increased Arabidopsis aluminum resistance and improved carbon-use efficiency for aluminum resistance. *Plant J.* **2012**, *71*, 327–337. [[CrossRef](#)] [[PubMed](#)]
23. Ding, Z.; Yan, J.; Xu, X.; Li, G.; Zheng, S. WRKY46 functions as a transcriptional repressor of ALMT1, regulating aluminum-induced malate secretion in Arabidopsis. *Plant J.* **2013**, *76*, 825–835. [[CrossRef](#)] [[PubMed](#)]
24. Li, G.; Wang, Z.; Yokosho, K.; Ding, B.; Fan, W.; Gong, Q.; Li, G.; Wu, Y.; Yang, J.; Ma, J. Transcription factor WRKY22 promotes aluminum tolerance via activation of *OsFRDL4* expression and enhancement of citrate secretion in rice (*Oryza sativa*). *New Phytol.* **2018**, *219*, 149–162. [[CrossRef](#)] [[PubMed](#)]
25. Iuchi, S.; Koyama, H.; Iuchi, A.; Kobayashi, Y.; Kitabayashi, S.; Kobayashi, Y.; Ikka, T.; Hirayama, T.; Shinozaki, K.; Kobayashi, M. Zinc finger protein STOP1 is critical for proton tolerance in *Arabidopsis* and coregulates a key gene in aluminum tolerance. *Proc. Natl. Acad. Sci. USA* **2007**, *104*, 9900–9905. [[CrossRef](#)] [[PubMed](#)]
26. Iuchi, S.; Kobayashi, Y.; Koyama, H.; Kobayashi, M. STOP1, a Cys2/His2 type zinc-finger protein, plays critical role in acid soil tolerance in Arabidopsis. *Plant Signal Behav.* **2008**, *3*, 128–130. [[CrossRef](#)] [[PubMed](#)]
27. Sawaki, Y.; Iuchi, S.; Kobayashi, Y.; Kobayashi, Y.; Ikka, T.; Sakurai, N.; Fujita, M.; Shinozaki, K.; Shibata, D.; Kobayashi, M.; et al. STOP1 regulates multiple genes that protect Arabidopsis from proton and aluminum toxicities. *Plant Physiol.* **2009**, *150*, 281–294. [[CrossRef](#)]
28. Sawaki, Y.; Kobayashi, Y.; Kihara-Doi, T.; Nishikubo, N.; Kawazu, T.; Kobayashi, M.; Kobayashi, Y.; Iuchi, S.; Koyama, H.; Sato, S. Identification of a STOP1-like protein in Eucalyptus that regulates transcription of Al tolerance genes. *Plant Sci.* **2014**, *223*, 8–15. [[CrossRef](#)]
29. Kobayashi, Y.; Ohyama, Y.; Kobayashi, Y.; Ito, H.; Iuchi, S.; Fujita, M.; Zhao, C.; Tanveer, T.; Ganesan, M.; Kobayashi, M.; et al. STOP2 activates transcription of several genes for Al- and low pH-tolerance that are regulated by STOP1 in Arabidopsis. *Mol. Plant* **2014**, *7*, 311–322. [[CrossRef](#)]
30. Ohyama, Y.; Ito, H.; Kobayashi, Y.; Ikka, T.; Morita, A.; Kobayashi, M.; Imaizumi, R.; Aoki, T.; Komatsu, K.; Sakata, Y.; et al. Characterization of *AtSTOP1* orthologous genes in tobacco and other plant species. *Plant Physiol.* **2013**, *162*, 1937–1946. [[CrossRef](#)]
31. Huang, S.; Gao, J.; You, J.; Liang, Y.; Guan, K.; Yan, S.; Zhan, M.; Yang, Z. Identification of STOP1-like proteins associated with aluminum tolerance in sweet sorghum (*Sorghum bicolor* L.). *Front. Plant Sci.* **2018**, *9*, 258. [[CrossRef](#)] [[PubMed](#)]
32. Wu, W.; Lin, Y.; Chen, Q.; Peng, W.; Peng, J.; Tian, J.; Liang, Q.; Liao, H. Functional conservation and divergence of soybean *GmSTOP1* members in proton and aluminum tolerance. *Front. Plant Sci.* **2018**, *9*, 570. [[CrossRef](#)] [[PubMed](#)]
33. Krasnov, G.S.; Dmitriev, A.A.; Zyablitsin, A.V.; Rozhmina, T.A.; Zhuchenko, A.A.; Kezimana, P.; Snezhkina, A.V.; Fedorova, M.S.; Novakovskiy, R.O.; Pushkova, E.N.; et al. Aluminum responsive genes in Flax (*Linum usitatissimum* L.). *Biomed. Res. Int.* **2019**, *2019*, 5023125. [[CrossRef](#)] [[PubMed](#)]
34. Yanofsky, M.F.; Ma, H.; Bowman, J.L.; Drews, G.N.; Feldmann, K.A.; Meyerowitz, E.M. The protein encoded by the Arabidopsis homeotic gene *agamous* resembles transcription factors. *Nature* **1990**, *346*, 35–39. [[CrossRef](#)] [[PubMed](#)]
35. Becker, A.; Theissen, G. The major clades of MADS-box genes and their role in the development and evolution of flowering plants. *Mol. Phylogenet Evol.* **2003**, *29*, 464–489. [[CrossRef](#)]
36. Fan, C.; Wang, X.; Wang, Y.; Hu, R.; Zhang, X.; Chen, J.; Fu, Y. Genome-wide expression analysis of soybean MADS genes showing potential function in the seed development. *PLoS ONE* **2013**, *8*, e62288. [[CrossRef](#)]
37. Alvarez-Buylla, E.R.; Pelaz, S.; Liljegren, S.J.; Gold, S.E.; Burgeff, C.; Ditta, G.S.; Ribas de Pouplana, L.; Martinez-Castilla, L.; Yanofsky, M.F. An ancestral MADS-box gene duplication occurred before the divergence of plants and animals. *Proc. Natl. Acad. Sci. USA* **2000**, *97*, 5328–5333. [[CrossRef](#)]

38. Kaufmann, K.; Melzer, R.; Theissen, G. MIKC-type MADS-domain proteins: Structural modularity, protein interactions and network evolution in land plants. *Gene* **2005**, *347*, 183–198. [[CrossRef](#)]
39. Theissen, G.; Kim, J.T.; Saedler, H. Classification and phylogeny of the MADS-box multigene family suggest defined roles of MADS-box gene subfamilies in the morphological evolution of eukaryotes. *J. Mol. Evol.* **1996**, *43*, 484–516. [[CrossRef](#)]
40. De Bodt, S.; Raes, J.; Florquin, K.; Rombauts, S.; Rouze, P.; Theissen, G.; Van de Peer, Y. Genomewide structural annotation and evolutionary analysis of the type I MADS-box genes in plants. *J. Mol. Evol.* **2003**, *56*, 573–586. [[CrossRef](#)]
41. Ng, M.; Yanofsky, M.F. Function and evolution of the plant MADS-box gene family. *Nat. Rev. Genet.* **2001**, *2*, 186–195. [[CrossRef](#)] [[PubMed](#)]
42. Ratcliffe, O.J.; Nadzan, G.C.; Reuber, T.L.; Riechmann, J.L. Regulation of flowering in Arabidopsis by an FLC homologue. *Plant Physiol.* **2001**, *126*, 122–132. [[CrossRef](#)] [[PubMed](#)]
43. Yang, Y.; Fanning, L.; Jack, T. The K domain mediates heterodimerization of the Arabidopsis floral organ identity proteins, APETALA3 and PISTILLATA. *Plant J.* **2003**, *33*, 47–59. [[CrossRef](#)] [[PubMed](#)]
44. Honma, T.; Goto, K. Complexes of MADS-box proteins are sufficient to convert leaves into floral organs. *Nature* **2001**, *409*, 525–529. [[CrossRef](#)] [[PubMed](#)]
45. Pelaz, S.; Gustafson-Brown, C.; Kohalmi, S.E.; Crosby, W.L.; Yanofsky, M.F. APETALA1 and SEPALLATA3 interact to promote flower development. *Plant J.* **2001**, *26*, 385–394. [[CrossRef](#)] [[PubMed](#)]
46. Lamb, R.S.; Irish, V.F. Functional divergence within the APETALA3/PISTILLATA floral homeotic gene lineages. *Proc. Natl. Acad. Sci. USA* **2003**, *100*, 6558–6563. [[CrossRef](#)]
47. Kaufmann, K.; Pajoro, A.; Angenent, G.C. Regulation of transcription in plants: Mechanisms controlling developmental switches. *Nat. Rev. Genet.* **2010**, *11*, 830–842. [[CrossRef](#)]
48. Theissen, G. Development of floral organ identity: Stories from the MADS house. *Curr. Opin. Plant Biol.* **2001**, *4*, 75–85. [[CrossRef](#)]
49. Hepworth, S.R.; Valverde, F.; Ravenscroft, D.; Mouradov, A.; Coupland, G. Antagonistic regulation of flowering-time gene SOC1 by CONSTANS and FLC via separate promoter motifs. *Embo J.* **2002**, *21*, 4327–4337. [[CrossRef](#)]
50. Zhang, L.; Xu, Y.; Ma, R. Molecular cloning, identification, and chromosomal localization of two MADS box genes in peach (*Prunus persica*). *J. Genet. Genom.* **2008**, *35*, 365–372. [[CrossRef](#)]
51. Moyle, R.; Fairbairn, D.J.; Ripi, J.; Crowe, M.; Botella, J.R. Developing pineapple fruit has a small transcriptome dominated by metallothionein. *J. Exp. Bot.* **2005**, *56*, 101–112. [[CrossRef](#)] [[PubMed](#)]
52. Zheng, Y.; Ren, N.; Wang, H.; Stromberg, A.J.; Perry, S.E. Global identification of targets of the Arabidopsis MADS domain protein AGAMOUS-Like15. *Plant Cell* **2009**, *21*, 2563–2577. [[CrossRef](#)] [[PubMed](#)]
53. Battaglia, R.; Brambilla, V.; Colombo, L.; Stuitje, A.R.; Kater, M.M. Functional analysis of MADS-box genes controlling ovule development in Arabidopsis using the ethanol-inducible alc gene-expression system. *Mech. Dev.* **2006**, *123*, 267–276. [[CrossRef](#)] [[PubMed](#)]
54. Ferrario, S.; Shchennikova, A.V.; Franken, J.; Immink, R.G.; Angenent, G.C. Control of floral meristem determinacy in petunia by MADS-box transcription factors. *Plant Physiol.* **2006**, *140*, 890–898. [[CrossRef](#)]
55. Alvarez-Buylla, E.R.; Liljegren, S.J.; Pelaz, S.; Gold, S.E.; Burgeff, C.; Ditta, G.S.; Vergara-Silva, F.; Yanofsky, M.F. MADS-box gene evolution beyond flowers: Expression in pollen, endosperm, guard cells, roots and trichomes. *Plant J.* **2000**, *24*, 457–466. [[CrossRef](#)]
56. Ambrose, B.A.; Lerner, D.R.; Ciceri, P.; Padilla, C.M.; Yanofsky, M.F.; Schmidt, R.J. Molecular and genetic analyses of the *silky1* gene reveal conservation in floral organ specification between eudicots and monocots. *Mol. Cell* **2000**, *5*, 569–579. [[CrossRef](#)]
57. Zhao, H.; Jia, H.; Wang, Y.; Wang, G.; Zhou, C.; Jia, H.; Gao, Z. Genome-wide identification and analysis of the MADS-box gene family and its potential role in fruit development and ripening in red bayberry (*Morella rubra*). *Gene* **2019**, *717*, 144045. [[CrossRef](#)]
58. Jiao, Y.; Yin, H.; Chen, Y.; Gao, M.; Wu, L.; Wang, Y. Ectopic expression of *Litsea cubeba* LcMADS20 modifies siliqua architecture. *G3 (Bethesda)* **2019**, *9*, 4139–4147. [[CrossRef](#)]

59. Yin, X.; Liu, X.; Xu, B.; Lu, P.; Dong, T.; Yang, D.; Ye, T.; Feng, Y.; Wu, Y. OsMADS18, a membrane-bound MADS-box transcription factor, modulates plant architecture and the abscisic acid response in rice. *J. Exp. Bot.* **2019**, *70*, 3895–3909. [[CrossRef](#)]
60. Teo, Z.; Zhou, W.; Shen, L. Dissecting the function of MADS-box transcription factors in orchid reproductive development. *Front. Plant Sci.* **2019**, *10*, 1474. [[CrossRef](#)]
61. Bai, S.; Liu, Y.; Sun, J.; Zhu, L. Molecular mapping of split rice spikelet mutant srs-1 and analysis of its homeotic function in rice. *Sci. China C Life Sci.* **2000**, *43*, 369–375. [[CrossRef](#)] [[PubMed](#)]
62. Lozano, R.; Angosto, T.; Gomez, P.; Payan, C.; Capel, J.; Huijser, P.; Salinas, J.; Martinez-Zapater, J.M. Tomato flower abnormalities induced by low temperatures are associated with changes of expression of MADS-Box genes. *Plant Physiol.* **1998**, *117*, 91–100. [[CrossRef](#)] [[PubMed](#)]
63. Lee, S.; Choi, S.C.; An, G. Rice SVP-group MADS-box proteins, OsMADS22 and OsMADS55, are negative regulators of brassinosteroid responses. *Plant J.* **2008**, *54*, 93–105. [[CrossRef](#)] [[PubMed](#)]
64. Chen, C.; Begcy, K.; Liu, K.; Folsom, J.J.; Wang, Z.; Zhang, C.; Walia, H. Heat stress yields a unique MADS box transcription factor in determining seed size and thermal sensitivity. *Plant Physiol.* **2016**, *171*, 606–622. [[CrossRef](#)]
65. Chen, R.; Ma, J.; Luo, D.; Hou, X.; Ma, F.; Zhang, Y.; Meng, Y.; Zhang, H.; Guo, W. CaMADS, a MADS-box transcription factor role in the response to cold, salt and osmotic stress. *Plant Sci.* **2019**, *280*, 164–174. [[CrossRef](#)]
66. Arora, R.; Agarwal, P.; Ray, S.; Singh, A.K.; Singh, V.P.; Tyagi, A.K.; Kapoor, S. MADS-box gene family in rice: Genome-wide identification, organization and expression profiling during reproductive development and stress. *Bmc Genom.* **2007**, *8*, 242. [[CrossRef](#)]
67. Puig, J.; Meynard, D.; Khong, G.N.; Pauluzzi, G.; Guiderdoni, E.; Gantet, P. Analysis of the expression of the AGL17-like clade of MADS-box transcription factors in rice. *Gene Expr. Patterns* **2013**, *13*, 160–170. [[CrossRef](#)]
68. Wei, B.; Zhang, R.Z.; Guo, J.J.; Liu, D.M.; Li, A.L.; Fan, R.C.; Mao, L.; Zhang, X.Q. Genome-wide analysis of the MADS-box gene family in *Brachypodium distachyon*. *PLoS ONE* **2014**, *9*, e84781. [[CrossRef](#)]
69. Duan, W.; Song, X.; Liu, T.; Huang, Z.; Ren, J.; Hou, X.; Li, Y. Genome-wide analysis of the MADS-box gene family in *Brassica rapa* (Chinese cabbage). *Mol. Genet. Genom.* **2015**, *290*, 239–255. [[CrossRef](#)]
70. Saha, G.; Park, J.; Jung, H.; Ahmed, N.U.; Kayum, M.A.; Chung, M.; Hur, Y.; Cho, Y.; Watanabe, M.; Nou, I. Genome-wide identification and characterization of MADS-box family genes related to organ development and stress resistance in *Brassica rapa*. *Bmc Genom.* **2015**, *16*, 178. [[CrossRef](#)]
71. Ma, J.; Yang, Y.; Luo, W.; Yang, C.; Ding, P.; Liu, Y.; Qiao, L.; Chang, Z.; Geng, H.; Wang, P.; et al. Genome-wide identification and analysis of the MADS-box gene family in bread wheat (*Triticum aestivum* L.). *PLoS ONE* **2017**, *12*, e181443. [[CrossRef](#)] [[PubMed](#)]
72. Shu, Y.; Yu, D.; Wang, D.; Guo, D.; Guo, C. Genome-wide survey and expression analysis of the MADS-box gene family in soybean. *Mol. Biol. Rep.* **2013**, *40*, 3901–3911. [[CrossRef](#)] [[PubMed](#)]
73. Wu, C.; Ma, Q.; Yam, K.M.; Cheung, M.Y.; Xu, Y.; Han, T.; Lam, H.M.; Chong, K. In situ expression of the *GmNMH7* gene is photoperiod-dependent in a unique soybean (*Glycine max* [L.] Merr.) flowering reversion system. *Planta* **2006**, *223*, 725–735. [[CrossRef](#)] [[PubMed](#)]
74. Thakare, D.; Tang, W.; Hill, K.; Perry, S.E. The MADS-domain transcriptional regulator AGAMOUS-LIKE15 promotes somatic embryo development in Arabidopsis and soybean. *Plant Physiol.* **2008**, *146*, 1663–1672. [[CrossRef](#)] [[PubMed](#)]
75. Huang, F.; Xu, G.; Chi, Y.; Liu, H.; Xue, Q.; Zhao, T.; Gai, J.; Yu, D. A soybean MADS-box protein modulates floral organ numbers, petal identity and sterility. *Bmc Plant Biol.* **2014**, *14*, 89. [[CrossRef](#)] [[PubMed](#)]
76. Huang, F.; Chi, Y.; Gai, J.; Yu, D. Identification of transcription factors predominantly expressed in soybean flowers and characterization of GmSEP1 encoding a SEPALLATA1-like protein. *Gene* **2009**, *438*, 40–48. [[CrossRef](#)]
77. Xu, J.; Zhong, X.; Zhang, Q.; Li, H. Overexpression of the *GmGAL2* gene accelerates flowering in Arabidopsis. *Plant Mol. Biol. Report.* **2010**, *28*, 704–711. [[CrossRef](#)]
78. Chi, Y.; Wang, T.; Xu, G.; Yang, H.; Zeng, X.; Shen, Y.; Yu, D.; Huang, F. *GmAGL1*, a MADS-box gene from soybean, is involved in floral organ identity and fruit dehiscence. *Front. Plant Sci.* **2017**, *8*, 175. [[CrossRef](#)]

79. Zeng, X.; Liu, H.; Du, H.; Wang, S.; Yang, W.; Chi, Y.; Wang, J.; Huang, F.; Yu, D. Soybean MADS-box gene *GmAGL1* promotes flowering via the photoperiod pathway. *Bmc Genom.* **2018**, *19*, 51. [[CrossRef](#)]
80. Ping, J.; Liu, Y.; Sun, L.; Zhao, M.; Li, Y.; She, M.; Sui, Y.; Lin, F.; Liu, X.; Tang, Z.; et al. *Dt2* is a gain-of-function MADS-domain factor gene that specifies semideterminacy in soybean. *Plant Cell* **2014**, *26*, 2831–2842. [[CrossRef](#)]
81. Zheng, Q.; Zheng, Y.; Perry, S.E. Decreased *GmAGL15* expression and reduced ethylene synthesis may contribute to reduced somatic embryogenesis in a poorly embryogenic cultivar of *Glycine max*. *Plant Signal. Behav.* **2013**, *8*, e25422. [[CrossRef](#)] [[PubMed](#)]
82. Zheng, Q.; Perry, S.E. Alterations in the transcriptome of soybean in response to enhanced somatic embryogenesis promoted by orthologs of AGAMOUS-Like 15 and AGAMOUS-Like 18. *Plant Physiol.* **2014**, *164*, 1365–1377. [[CrossRef](#)] [[PubMed](#)]
83. Perry, S.E.; Zheng, Q.; Zheng, Y. Transcriptome analysis indicates that *GmAGAMOUS-Like 15* may enhance somatic embryogenesis by promoting a dedifferentiated state. *Plant Signal. Behav.* **2016**, *11*, e1197463. [[CrossRef](#)] [[PubMed](#)]
84. Wong, C.E.; Singh, M.B.; Bhalla, P.L. Novel members of the AGAMOUS LIKE 6 subfamily of MIKCC-type MADS-box genes in soybean. *Bmc Plant Biol.* **2013**, *13*, 105. [[CrossRef](#)] [[PubMed](#)]
85. Jia, Z.; Jiang, B.; Gao, X.; Yue, Y.; Fei, Z.; Sun, H.; Wu, C.; Sun, S.; Hou, W.; Han, T. *GmFULa*, a FRUITFULL homolog, functions in the flowering and maturation of soybean. *Plant Cell Rep.* **2015**, *34*, 121–132. [[CrossRef](#)]
86. Na, X.; Jian, B.; Yao, W.; Wu, C.; Hou, W.; Jiang, B.; Bi, Y.; Han, T. Cloning and functional analysis of the flowering gene *GmSOC1-like*, a putative SUPPRESSOR OF OVEREXPRESSION CO1/AGAMOUS-LIKE 20 (SOC1/AGL20) ortholog in soybean. *Plant Cell Rep.* **2013**, *32*, 1219–1229. [[CrossRef](#)]
87. Zhang, H.; Forde, B.G. An Arabidopsis MADS box gene that controls nutrient-induced changes in root architecture. *Science* **1998**, *279*, 407–409. [[CrossRef](#)]
88. Gan, Y.; Filleur, S.; Rahman, A.; Gotensparre, S.; Forde, B.G. Nutritional regulation of ANR1 and other root-expressed MADS-box genes in *Arabidopsis thaliana*. *Planta* **2005**, *222*, 730–742. [[CrossRef](#)]
89. Zeng, Q.; Yang, C.; Ma, Q.; Li, X.; Dong, W.; Nian, H. Identification of wild soybean miRNAs and their target genes responsive to aluminum stress. *BMC Plant Biol.* **2012**, *12*, 182. [[CrossRef](#)]
90. Liu, W.; Han, X.; Zhan, G.; Zhao, Z.; Feng, Y.; Wu, C. A novel sucrose-regulatory MADS-box transcription factor *GmNMHC5* promotes root development and nodulation in soybean (*Glycine max* [L.] Merr.). *Int. J. Mol. Sci.* **2015**, *16*, 20657–20673. [[CrossRef](#)] [[PubMed](#)]
91. Ma, Q.; Yi, R.; Li, L.; Liang, Z.; Zeng, T.; Zhang, Y.; Huang, H.; Zhang, X.; Yin, X.; Cai, Z.; et al. GsMATE encoding a multidrug and toxic compound extrusion transporter enhances aluminum tolerance in *Arabidopsis thaliana*. *Bmc Plant Biol.* **2018**, *18*, 212. [[CrossRef](#)] [[PubMed](#)]
92. Lü, J.; Suo, H.; Yi, R.; Ma, Q.; Nian, H. *Glyma11g13220*, a homolog of the vernalization pathway gene *VERNALIZATION 1* from soybean [*Glycine max* (L.) Merr.], promotes flowering in *Arabidopsis thaliana*. *BMC Plant Biol.* **2015**, *15*, 232. [[CrossRef](#)] [[PubMed](#)]
93. Giannakoula, A.; Moustakas, M.; Mylona, P.; Papadakis, I.; Yupsanis, T. Aluminum tolerance in maize is correlated with increased levels of mineral nutrients, carbohydrates and proline, and decreased levels of lipid peroxidation and Al accumulation. *J. Plant Physiol.* **2008**, *165*, 385–396. [[CrossRef](#)] [[PubMed](#)]
94. Gan, Y.; Bernreiter, A.; Filleur, S.; Abram, B.; Forde, B.G. Overexpressing the ANR1 MADS-box gene in transgenic plants provides new insights into its role in the nitrate regulation of root development. *Plant Cell Physiol.* **2012**, *53*, 1003–1016. [[CrossRef](#)]
95. Ma, Q.; Xia, Z.; Cai, Z.; Li, L.; Cheng, Y.; Liu, J.; Nian, H. *GmWRKY16* enhances drought and salt tolerance through an ABA-mediated pathway in *Arabidopsis thaliana*. *Front. Plant Sci.* **2019**, *9*, 1979. [[CrossRef](#)]
96. Godon, C.; Mercier, C.; Wang, X.; David, P.; Richaud, P.; Nussaume, L.; Liu, D.; Desnos, T. Under phosphate starvation conditions, Fe and Al trigger accumulation of the transcription factor STOP1 in the nucleus of *Arabidopsis* root cells. *Plant J.* **2019**, *99*, 937–949. [[CrossRef](#)]
97. Liang, C.; Pinos, M.A.; Tian, J.; Yao, Z.; Sun, L.; Liu, J.; Shaff, J.; Coluccio, A.; Kochian, L.V.; Liao, H. Low pH, aluminum, and phosphorus coordinately regulate malate exudation through *GmALMT1* to improve soybean adaptation to acid soils. *Plant Physiol.* **2013**, *161*, 1347–1361. [[CrossRef](#)]

98. Suo, H.; Ma, Q.; Ye, K.; Yang, C.; Tang, Y.; Hao, J.; Zhang, Z.J.; Chen, M.; Feng, Y.; Nian, H. Overexpression of *AtDREB1A* causes a severe dwarf phenotype by decreasing endogenous gibberellin levels in soybean [*Glycine max* (L.) Merr.]. *PLoS ONE* **2012**, *7*, e45568. [[CrossRef](#)]
99. Clough, S.J.; Bent, A.F. Floral dip: A simplified method for *Agrobacterium*-mediated transformation of *Arabidopsis thaliana*. *Plant J.* **1998**, *16*, 735–743.
100. Collins, T.J. Image J for microscopy. *BioTechniques* **2007**, *43*, 25–30.



© 2020 by the authors. Licensee MDPI, Basel, Switzerland. This article is an open access article distributed under the terms and conditions of the Creative Commons Attribution (CC BY) license (<http://creativecommons.org/licenses/by/4.0/>).